

Low energy magnetic excitations in the spin-orbital Mott insulator Sr_2IrO_4

S. Bahr,¹ A. Alfonsov,¹ G. Jackeli,² G. Khaliullin,² A. Matsumoto,³
T. Takayama,² H. Takagi,^{3,2} B. Büchner,^{1,4} and V. Kataev¹

¹*Leibniz Institute for Solid State and Materials Research IFW Dresden, D-01171 Dresden, Germany*

²*Max Planck Institute for Solid State Research, Heisenbergstrasse 1, D-70569 Stuttgart, Germany*

³*Department of Physics and Department of Advanced Materials, University of Tokyo, Hongo 113-0033, Japan*

⁴*Institut für Festkörperphysik, Technische Universität Dresden, D-01062 Dresden, Germany*

(Dated: June 15, 2021)

We report a high-field electron spin resonance study in the sub-THz frequency domain of a single crystal of Sr_2IrO_4 that has been recently proposed as a prototypical spin-orbital Mott insulator. In the antiferromagnetically (AFM) ordered state with noncollinear spin structure that occurs in this material at $T_N \approx 240$ K we observe both the "low" frequency mode due to the precession of weak ferromagnetic moments arising from a spin canting, and the "high" frequency modes due to the precession of the AFM sublattices. Surprisingly, the energy gap for the AFM excitations appears to be very small, amounting to 0.83 meV only. This suggests a rather isotropic Heisenberg dynamics of interacting Ir^{4+} effective spins despite the spin-orbital entanglement in the ground state.

PACS numbers: 75.30.-m, 75.50.Ee, 76.30.-v

Many $3d$ transition metal oxides (TMOs) such as parent compounds of the cuprate high-temperature superconductors are insulators despite a partial filling of the d shell. The Mott (or charge transfer) gap of the order of several eV opens in the $3d$ band due to a strong on-site Coulomb repulsion of electrons U , rendering these materials magnetic insulators (for a review see, e.g., Ref. [1]). In $5d$ TMOs the d shell is more extended in space yielding a stronger overlap of the orbitals which favors electron delocalization and reduces U . Nevertheless, an insulating magnetic ground state still often occurs, e.g., in complex Ir oxides. One striking example is Sr_2IrO_4 which is analogous (see Fig. 1) from the viewpoint of crystallographic [2] and magnetic structure [3] to the celebrated two-dimensional (2D) spin-1/2 Heisenberg quantum antiferromagnet La_2CuO_4 . A recent study of the electronic structure of Sr_2IrO_4 [4] has shown that the insulating state arises due to a strong spin-orbit coupling (SOC) of the order of 0.5 eV that gives rise to a narrow half-filled band characterized by the effective total angular momentum $J_{\text{eff}} = 1/2$. Even a small U opens the Mott gap of ~ 0.5 eV in this band [4, 5]. In contrast to the cuprates, the driving force for the insulating state in Sr_2IrO_4 is the SOC which suggests this material as a novel kind of spin-orbital Mott insulator [3, 4]. On the atomic level, a coupling of the spin and orbital momentum in Ir^{4+} ion yields a Kramers doublet with the effective spin $J_{\text{eff}} = 1/2$ which however has very different properties as compared to the real spin-1/2 state in La_2CuO_4 . Recent theories suggest that the entanglement of the spin and orbital momentum in Ir oxides can lead to a rich diversity of magnetic ground states, ranging from a "conventional" Néel antiferromagnetic (AFM) state, to stripe AFM phases and to a spin-liquid regime [6–8]. In Sr_2IrO_4 the J_{eff} spins AFM order in the ab plane below $T_N \approx 240$ K. Owing to the admixture of the orbital

moment the effective spins follow the rotation of the IrO octahedra which yields noncollinearity of the spin sublattices [3] (Fig. 1). The value of the in-plane ferromagnetic (FM) moment $M_{\text{FM}} \sim 0.06 - 0.1 \mu_{\text{B}}/\text{Ir}$ [2, 3, 9, 10], which arises due to the Dzyaloshinskii-Moriya (DM) interaction, is much larger than in La_2CuO_4 , as expected because of the strong SOC. Surprisingly, dynamic correlations of J_{eff} spins in the paramagnetic state of Sr_2IrO_4 reveal isotropic 2D Heisenberg behavior despite the strong entanglement of spins and orbitals [10].

The low energy dynamics of effective spins in Sr_2IrO_4 below T_N has not been yet sufficiently addressed. Inelastic neutron scattering experiments are complicated by a strong absorption of neutrons by Ir and, to our knowledge, have not been reported so far. The magnon dispersion has been recently measured by the resonant inelastic x-ray scattering (RIXS) [11]. However a limited energy resolution did not enable to resolve a possible gap in the excitation spectrum which could arise due to the SOC. In this situation electron spin resonance (ESR) spectroscopy, with its very high energy resolution down to $\sim \mu\text{eV}$ and extreme sensitivity to magnetic anisotropies, could provide fundamental insights into properties of the magnetic excitations in spin-orbital Mott insulators. In the present work we study the low-energy spin dynamics in single crystals of Sr_2IrO_4 in the AFM ordered state with the ESR technique in a broad frequency range up to 500 GHz. We have identified both the ferromagnetic-like resonance mode, associated with the precession of the DM moments, and the AFM resonance (AFMR) modes due to the resonant excitation of the AFM sublattices. The latter modes reveal a very small spin wave gap $\Delta = 0.83$ meV which is just a fraction of that observed in La_2CuO_4 . Indeed, it would not be possible to resolve such a small gap in the RIXS experiment [11]. Our observation of practically gapless excitations of effective J_{eff}

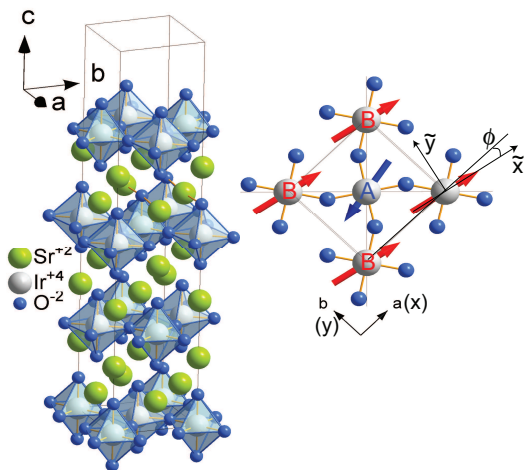


FIG. 1. (Color online) Left: crystallographic unit cell of Sr_2IrO_4 . Right: the ordering pattern of effective Ir spins $J_{\text{eff}} = 1/2$ in the ab crystallographic plane [3]. The spin in the center and its four neighbors belong to the two AFM sublattices, A and B respectively, canted by an angle ϕ .

spins in the spin-orbital Mott insulator is remarkable. It appears that, in the magnetic sector, despite the spin-orbital entanglement Sr_2IrO_4 shows the behavior of a quasi-2D Heisenberg antiferromagnet.

The growth and characterization of single crystals of Sr_2IrO_4 have been described in Ref. [3]. ESR measurements have been performed with a commercial Bruker EMX spectrometer at a fixed frequency $\nu \sim 10$ GHz, at fields up to 1 T and with a home-made multi-frequency high-field ESR (HF-ESR) spectrometer at fields up to 14 T and ν up to 500 GHz [12]. In the latter case a highly sensitive quasi-optical detection scheme in the so-called induction mode without resonance cavities has been employed [13, 14].

In the AFM ordered IrO_2 plane of Sr_2IrO_4 a net ferromagnetic moment arises due to the DM interaction. These FM (or DM) moments are AFM coupled along the c axis in the up-down-down-up ($\uparrow\downarrow\downarrow\uparrow$) arrangement [3]. Application of the in-plane magnetic field above the critical value H_c yields a metamagnetic transition from the AFM to a weakly FM state with $\mu_0 H_c$ increasing up to ~ 0.2 T at low temperatures [3, 9]. Therefore, as is generally expected for a canted two-sublattice antiferromagnet with "hidden" ferromagnetism, there should be a low-frequency ferromagnetic resonance (FMR) mode that represents the oscillation of the net FM moment around its equilibrium position and a high-frequency mode that arises due to the precession of the AFM sublattices [15–18]. Though qualitatively similar to the case of collinear AFM lattices, the latter resonance mode is renormalized by the DM interaction (see Refs. [15–18] and the discussion below).

Experimentally, we observe the FMR mode in Sr_2IrO_4 at fields above H_c by measuring the ESR with a 10 GHz

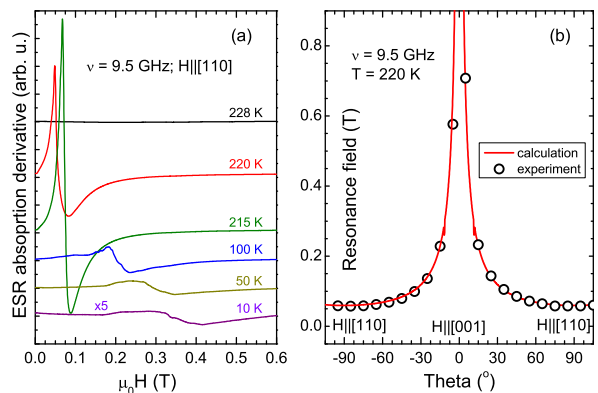


FIG. 2. (Color online) (a) FMR signal at $\nu = 9.5$ GHz at selected temperatures below T_N for the in-plane orientation of the magnetic field; (b) orientational dependence of the FMR resonance field at $\nu = 9.5$ GHz and $T = 220$ K (circles). Solid line shows $1/\sin\theta$ fit (see text).

setup. As illustrated by Fig. 2(a) for the magnetic field geometry $\mathbf{H}||[110]$, the signal appears right below the AFM phase transition. (Note that in this setup the detected signal is the field derivative of the microwave absorption). The resonance field H_{res} shifts to higher fields with lowering the temperature, the resonance line first grows in amplitude, however, below ~ 100 K the signal substantially broadens and acquires an additional structure. In classical FMR theories the increase of H_{res} should be related with a decrease of the effective DM field which enters the resonance conditions and is responsible for the downshift of the FMR mode from the paramagnetic resonance value [18]. Interestingly, after an initial rise below T_N the in-plane magnetization due to DM moments also decreases upon lowering the T at fields even exceeding H_c , as observed in our magnetization measurements (not shown) and also previously reported, e.g., in Ref. [19]. Furthermore, a distribution of internal fields in Sr_2IrO_4 has been observed below ~ 100 K in μSR experiments in Ref. [20]. It could be presumably assigned to the pinning of the DM moments by defects and be the reason for the broadening and structuring of the FMR mode at low T [Fig. 2(a)].

The rotation of the magnetic field from the in-plane ab orientation towards the c axis yields a strong shift of the FMR line to higher fields [Fig. 2(b)]. The angular dependence of resonance field at constant frequency follows perfectly a well known $1/\sin\theta$ law [solid line in Fig. 2(b)] characteristic for the low-frequency FMR mode [15].

The central result of our work is the observation of high-frequency AFMR modes in the HF-ESR measurements below T_N . Compared to the FMR signal, the AFM resonances are shifted up into the sub-THz frequency domain. As an example the AFMR signals at $T = 180$ K and $\mathbf{H}||[110]$ are shown in Fig. 3(a) for several selected frequencies. This mode reveals a very steep $\nu(H)$ de-

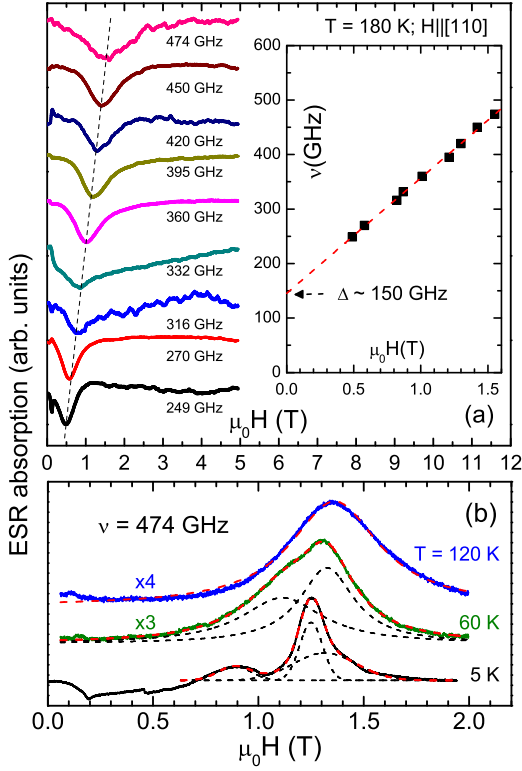


FIG. 3. (Color online) High-frequency AFMR mode for the in-plane orientation of the magnetic field. Upper panel: Characteristic frequency dependence at $T = 180$ K. The $\nu(H)$ AFMR resonance branch shown in the inset reveals a gap $\Delta \approx 150$ GHz. Bottom panel: Selected spectra at several temperatures for a fixed frequency $\nu = 474$ GHz. Dashed lines are the Lorentzian fits.

pendence with a frequency cutoff $\nu(H = 0) = 150$ GHz [Fig. 3(a), inset]. Similar to the behavior of the FMR mode, lowering the temperature below ~ 100 K yields the structuring of a single Lorentzian line into a group of overlapping resonances [Fig. 3(b)], again suggesting some distribution of internal fields in the sample. Nevertheless, all these closely lying resonances disperse in magnetic field very similar way and form a common $\nu(H)$ branch of excitations with an energy gap $\Delta \approx 200$ GHz ($= 0.83$ meV) at $T = 4$ K (Fig. 4). The AFM mode for $\mathbf{H} \parallel \mathbf{c}$ also acquires structure at low T but reveals a much shallower $\nu(H)$ dependence (Fig. 4). However, this AFM c -axis branch can be extrapolated to the same frequency cutoff Δ at zero field as the ab -plane branch.

With ESR one probes the AFM excitations in the center of the magnetic Brillouin zone, and the excitation gap Δ corresponds to the spin wave (SW) gap at the $q = 0$ wave vector [18]. We discuss the origin of this gap and its field dependencies based on an effective spin $S = 1/2$ model suggested for Sr_2IrO_4 in Ref. [6]. The model describes exchange interactions on intra-layer bonds of

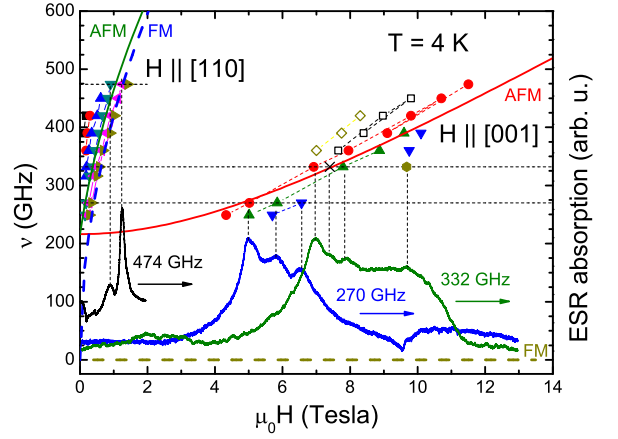


FIG. 4. (Color online) $\nu(H)$ diagram of the AFMR excitations in Sr_2IrO_4 at $T = 4$ K together with characteristic spectra for two directions of the magnetic field [symbols - experimental data points, solid lines - result of the modeling according to Eqs. (2) and (3). Thick dashed lines show the corresponding FMR modes. (see the text)]

neighboring iridium ions and has the form:

$$\mathcal{H}_{ij} = J\vec{S}_i \cdot \vec{S}_j + \Gamma S_i^z S_j^z + D(S_i^x S_j^y - S_i^y S_j^x). \quad (1)$$

Here the first term stands for isotropic AFM exchange (J), second and third terms describe symmetric (Γ) and antisymmetric (D) exchange anisotropies, respectively. We derive resonance frequencies within the linear SW theory. For the applied field H along the c -axis, the low-frequency FMR mode is gapless and field independent, and the high-frequency AFMR one is at energy

$$h\nu_c = \sqrt{32\tilde{J}\tilde{\Gamma}S^2 + (g_c\mu_B H)^2 / (1 - \tilde{\Gamma}/2\tilde{J})}. \quad (2)$$

Here, $\tilde{J} = \sqrt{J^2 + D^2}$ and $\tilde{\Gamma} = \tilde{J} - J - \Gamma > 0$ describe effective isotropic exchange and easy-plane anisotropy, respectively.

When the applied field is in ab -plane, both modes are gapped. Retaining the leading order contribution in H , we find the energy of AFMR mode

$$h\nu_{ab} \approx \sqrt{32\tilde{J}\tilde{\Gamma}S^2 + 4(2\tilde{J} + \tilde{\Gamma})M_{\text{FM}}H}, \quad (3)$$

where $M_{\text{FM}} = Sg_{ab}\mu_B \sin\phi$ is in-plane FM moment due to spin canting induced by DM interaction, and $\tan 2\phi = D/J$. The corresponding FMR mode $[(g_{ab}\mu_B H)^2 + 4(2\tilde{J} + \tilde{\Gamma})M_{\text{FM}}H]^{1/2}$ lies, in the high frequency domain, close to the AFMR one (Fig. 4). Considering the broadness of the high frequency ESR spectrum which at low T also features several overlapping resonances, it is difficult to distinguish there an FMR signal.

With $\tilde{J} \approx 100$ meV, as estimated in Ref. [10], and with the SW gap value $\Delta(H = 0) \approx 0.83$ meV (Fig. 4) one obtains from Eqs. (2) and (3) a surprisingly small value of the anisotropy exchange parameter $\tilde{\Gamma} = \Delta^2/8J \approx 1 \mu\text{eV}$.

Since $\tilde{J} \gg \tilde{\Gamma}$, the slope of the c axis AFMR $\nu(H)$ branch [Eq. 2] in fields $H > \Delta/g_c\mu_B$ is given mainly by the g factor. Therefore one can obtain the g_c value directly from the experimental data in Fig. 4 which yields $g_c \simeq 2.4$. A plot of Eq. (2) with these parameters is in a fairly good agreement with the experiment (Fig. 4). For the ab plane such direct determination of the g factor is not possible since the slope of the corresponding branch is strongly renormalized by the DM interaction induced in-plane FM moment M_{FM} , giving rise to a very steep $\nu(H)$ dependence [see Eq. (3) and Fig. 4]. With $M_{\text{FM}} \approx 0.06\mu_B$ [10] and the parameters estimated above, Eq. (3) gives satisfactory agreement with experimental data [Fig. 4].

The effective easy-plane anisotropy $\tilde{\Gamma}$, extracted above, appears to be surprisingly small, suggesting that the effects of the DM interaction D [see Eq. (1)], favoring in-plane canted spin order, and easy-axis anisotropy Γ , supporting collinear out-of-plane order, nearly compensate each other. This is a plausible scenario, requiring, however, “fine-tuning” of model parameters [6]. Alternatively, one may attribute the emergent tiny energy scale $\tilde{\Gamma}$ to weak inter-layer interactions and the observed modes to the antibonding states derived from single-layer in-plane FMR modes. However, within this second scenario we were not able to explain the field dependence of resonance frequency for $\mathbf{H}||\mathbf{c}$, see Fig. 4, as for this geometry single-layer in-plane FMR mode is gapless and field independent. Since the DM moments are confined to the basal plane the magnetic field dependence of the FMR mode is governed by the transverse component of the field $H_{\perp} = H \sin\theta$ only and vanishes in the parallel geometry [15, 16, 18]. For $\mathbf{H}||\mathbf{c}$, a weak inter-layer coupling $J' \ll J$ may only bring a weak field dependence of the modes derived from the in-plane FMR mode $h\nu_c^{\text{FM}} \sim (J'/J)g_c\mu_B H$, contrary to the observed nearly paramagnetic $h\nu_c^{\text{AFM}} \sim g_c\mu_B H$ behavior, as indeed expected from Eq. (2).

Our observation of the AFM excitations in Sr_2IrO_4 down to quite small frequencies despite the spin-orbital entangled nature of ground state doublet of iridium ion is striking. One would expect that an orbital contribution should, instead, give rise to a substantial magnetic anisotropy gap for the spin excitations. For comparison, the SW gap in the AFM state of La_2CuO_4 with a very similar magnetic structure and a similar exchange J amounts to $\Delta_{\text{LCO}} \sim 5 \text{ meV}$ (see., e.g., Ref. [21]). This copper oxide is considered to be nearly ideal realization of the Heisenberg $S = 1/2$ 2D quantum antiferromagnet due to an almost complete quenching of the orbital momentum of the Cu, and yet Δ_{LCO} appears to be several times larger than the gap $\Delta(H = 0) = 0.83 \text{ meV}$ in Sr_2IrO_4 . A similarly small gap has been observed by AFMR in another Cu-based canted quasi-2D Heisenberg antiferromagnet $\text{Cu}(\text{HCOO})_2 \cdot 4\text{H}_2\text{O}$ [22] where, however, the isotropic $J \approx 72 \text{ K}$ is by a factor $\sim 15 - 20$ smaller than in La_2CuO_4 and Sr_2IrO_4 . Given that the ratio

Δ/J is usually thought to increase with SOC, it is really surprising that $\Delta/J \sim 0.008$ in strong spin-orbit coupled Sr_2IrO_4 is much smaller than in weak SOC cuprates La_2CuO_4 ($\Delta/J \sim 0.04$) and $\text{Cu}(\text{HCOO})_2 \cdot 4\text{H}_2\text{O}$ ($\Delta/J \sim 0.07$). Remarkably, a recent resonant magnetic x-ray scattering study of Sr_2IrO_4 has revealed essentially isotropic Heisenberg-like behavior of dynamic magnetic correlations above T_N [10] quite similar to the behavior of La_2CuO_4 [23]. It is therefore plausible that below T_N such isotropic magnetic correlations result in a rather isotropic magnetic dynamics in Sr_2IrO_4 despite a strong entanglement of spin and orbital degrees of freedom. One should note a sizable antisymmetric DM anisotropy in Sr_2IrO_4 that leads to a “weak” FM moment of two orders of magnitude larger than that in La_2CuO_4 . However, the competition between antisymmetric and symmetric anisotropies (both being induced by the strong spin-orbit coupling and being sizable) may lead to a quasi-degeneracy of in-plane canted and out-of-plane collinear orders, thereby explaining an extremely small SW gap. The collinear c axis magnetic structure has indeed been observed in bilayer iridate $\text{Sr}_3\text{Ir}_2\text{O}_7$ [24] and in $\text{Sr}_2\text{Ir}_{0.9}\text{Mn}_{0.1}\text{O}_4$ [25].

In summary, we have studied by means of ESR the low energy dynamics of effective J_{eff} spins in the magnetically ordered state of the prototypical spin-orbital Mott insulator Sr_2IrO_4 . The observed resonance of the DM moments with its angular dependence can be well described by a standard phenomenological treatment of ferromagnetic resonance. In the sub-THz frequency domain we identify the resonance modes due to the oscillation of the AFM sublattices. Surprisingly, the AFMR branches reveal a very small spin wave gap at $H = 0$ amounting to $\sim 0.83 \text{ meV}$ only, far beyond the resolution limit of RIXS [11]. The smallness of the gap enables to classify Sr_2IrO_4 as an isotropic quasi-2D Heisenberg antiferromagnet, despite the spin-orbital entanglement in the ground state. Considering experimental constraints of the inelastic neutron scattering (strong neutron absorption) and RIXS (limited energy resolution), high-field high-frequency tunable ESR technique with its excellent energy resolution and very high sensitivity to magnetic anisotropies emerges as an instructive tool to study novel magnetic phases and low energy excitations in complex iridium based oxides.

This work has been supported in part by the Deutsche Forschungsgemeinschaft (DFG) through project FOR 912 “Coherence and relaxation of electron spins”.

-
- [1] M. Imada, A. Fujimori, and Y. Tokura, Rev. Mod. Phys. **70**, 1039 (1998).
 - [2] M. K. Crawford, M. A. Subramanian, R. L. Harlow, J. A. Fernandez-Baca, Z. R. Wang, and D. C. Johnston, Phys. Rev. B **49**, 9198 (1994).

- [3] B. J. Kim, H. Ohsumi, T. Komesu, S. Sakai, T. Morita, H. Takagi, and T. Arima, *Science* **323**, 1329 (2009).
- [4] B. J. Kim, H. Jin, S. J. Moon, J.-Y. Kim, B.-G. Park, C. S. Leem, J. Yu, T. W. Noh, C. Kim, S.-J. Oh, J.-H. Park, V. Durairaj, G. Cao, and E. Rotenberg, *Phys. Rev. Lett.* **101**, 076402 (2008).
- [5] S. J. Moon, H. Jin, W. S. Choi, J. S. Lee, S. S. A. Seo, J. Yu, G. Cao, T. W. Noh, and Y. S. Lee, *Phys. Rev. B* **80**, 195110 (2009).
- [6] G. Jackeli and G. Khaliullin, *Phys. Rev. Lett.* **102**, 017205 (2009).
- [7] J. Chaloupka, G. Jackeli, and G. Khaliullin, *Phys. Rev. Lett.* **105**, 027204 (2010).
- [8] W. Witczak-Krempa, G. Chen, Y. Kim, and L. Balents, *Annu. Rev. Condens. Matter Phys.* **5**, in press (2014), arXiv:1305.2193.
- [9] G. Cao, J. Bolivar, S. McCall, J. E. Crow, and R. P. Guertin, *Phys. Rev. B* **57**, R11039 (1998).
- [10] S. Fujiyama, H. Ohsumi, T. Komesu, J. Matsuno, B. J. Kim, M. Takata, T. Arima, and H. Takagi, *Phys. Rev. Lett.* **108**, 247212 (2012).
- [11] J. Kim, D. Casa, M. H. Upton, T. Gog, Y.-J. Kim, J. F. Mitchell, M. van Veenendaal, M. Daghofer, J. van den Brink, G. Khaliullin, and B. J. Kim, *Phys. Rev. Lett.* **108**, 177003 (2012).
- [12] C. Golze, A. Alfonsov, R. Klingeler, B. Büchner, V. Kataev, C. Mennerich, H.-H. Klauss, M. Goiran, J.-M. Broto, H. Rakoto, and et al., *Phys. Rev. B* **73**, 224403 (2006).
- [13] U. Schaufuss, V. Kataev, A. A. Zvyagin, B. Büchner, J. Sichelschmidt, J. Wykhoff, C. Krellner, C. Geibel, and F. Steglich, *Phys. Rev. Lett.* **102**, 076405 (2009).
- [14] M. R. Fuchs, T. F. Prisner, and K. Mobius, *Rev. Sci. Instrum.* **70**, 3681 (1999).
- [15] P. Pincus, *Phys. Rev. Lett.* **5**, 13 (1960).
- [16] H. J. Fink and D. Shaltiel, *Phys. Rev.* **130**, 627 (1963).
- [17] S. J. Williamson and S. Foner, *Phys. Rev.* **136**, A1102 (1964).
- [18] E. A. Turov, *Physical properties of magnetically ordered crystals*, edited by A. Tybulewicz and S. Chomet (Academic press New York and London, 1965).
- [19] S. Chikara, O. Korneta, W. P. Crummett, L. E. DeLong, P. Schlottmann, and G. Cao, *Phys. Rev. B* **80**, 140407 (2009).
- [20] I. Franke, P. J. Baker, S. J. Blundell, T. Lancaster, W. Hayes, F. L. Pratt, and G. Cao, *Phys. Rev. B* **83**, 094416 (2011).
- [21] B. Keimer, R. J. Birgeneau, A. Cassanho, Y. Endoh, M. Greven, M. A. Kastner, and G. Shirane, *Z. Phys. B* **91**, 373 (1993).
- [22] M. S. Seehra and T. G. Castner Jr., *Phys. Rev. B* **1**, 2289 (1970).
- [23] B. Keimer, N. Belk, R. J. Birgeneau, A. Cassanho, C. Y. Chen, M. Greven, M. A. Kastner, A. Aharony, Y. Endoh, R. W. Erwin, and G. Shirane, *Phys. Rev. B* **46**, 14034 (1992).
- [24] J. W. Kim, Y. Choi, J. Kim, J. F. Mitchell, G. Jackeli, M. Daghofer, J. van den Brink, G. Khaliullin, and B. J. Kim, *Phys. Rev. Lett.* **109**, 037204 (2012).
- [25] S. Calder, G.-X. Cao, M. D. Lumsden, J. W. Kim, Z. Gai, B. C. Sales, D. Mandrus, and A. D. Christianson, *Phys. Rev. B* **86**, 220403 (2012).